Bis-(−)-nor-meptazinols as Novel Nanomolar Cholinesterase Inhibitors with High Inhibitory Potency on Amyloid-β Aggregation

Qiong Xie,[†,#] Hao Wang,[‡,#] Zheng Xia,[‡] Meiyan Lu,[†] Weiwei Zhang,[‡] Xinghai Wang,[†] Wei Fu,[†] Yun Tang,[§] Wei Sheng,[†] Wei Li,[†] Wei Zhou,[‡] Xu Zhu,[‡] Zhuibai Qiu,*[,†] and Hongzhuan Chen*[,‡]

Department of Medicinal Chemistry, School of Pharmacy, Fudan University, 138 Yixueyuan Road, Shanghai 200032, P. R. China, Department of Pharmacology, Institute of Medical Sciences, Shanghai JiaoTong University School of Medicine, 280 South Chongqing Road, Shanghai 200025, P. R. China, and School of Pharmacy, East China University of Science and Technology, 130 Meilong Road, Shanghai 200237, P. R. China

Received February 9, 2007

Bis-(−)-nor-meptazinols (bis-(−)-nor-MEPs) **5** were designed and synthesized by connecting two (−)-nor-MEP monomers with alkylene linkers of different lengths via the secondary amino groups. Their acetylcholinesterase (AChE) inhibitory activities were more greatly influenced by the length of the alkylene chain than butyrylcholinesterase (BChE) inhibition. The most potent nonamethylene-tethered dimer **5h** exhibited low-nanomolar IC_{50} values for both ChEs, having a 10 000-fold and 1500-fold increase in inhibition of AChE and BChE compared with (−)-MEP. Molecular docking elucidated that **5h** simultaneously bound to the catalytic and peripheral sites in AChE via hydrophobic interactions with Trp86 and Trp286. In comparison, it folded in the large aliphatic cavity of BChE because of the absence of peripheral site and the enlargement of the active site. Furthermore, **5h** and **5i** markedly prevented the AChE-induced Aβ aggregation with IC_{50} values of 16.6 and 5.8 μM, similar to that of propidium (IC_{50} = 12.8 μM), which suggests promising disease-modifying agents for the treatment of AD patients.

Introduction

Alzheimer's disease (AD), which is characterized by progressive loss of memory and impairment in cognition,[1] is becoming a serious threat to life expectancy for elderly people. The main pathological changes in the AD brain are the abnormal formation of extracellular senile plaques consisting of aggregated amyloid-β-peptide (Aβ) deposits and intracellular neurofibrillary tangles (NTFs) consisting of abnormally phosphorylated microtubule-associated protein τ.[2]

Current clinical therapy for AD patients is mainly palliative treatment targeting acetylcholinesterase (AChE). On the basis of the cholinergic hypothesis,[3] inhibition of AChE effectively increases the available acetylcholine (ACh) within cholinergic synapses, resulting in modest improvement in cognitive symptoms. Mounting evidence has indicated that AChE may be involved in several noncholinergic functions.[4] AChE colocalizes with Aβ in senile plaques, promoting the assembly of Aβ into fibrils[5] and accelerating Aβ peptide deposition.[6] Structural models of the interaction between AChE and Aβ have recently been explored.[7] It has been speculated that AChE achieves its aggregation-promoting action through direct binding with Aβ via the specific region of the enzyme that involves a peripheral binding site.[8] Inhibition of the peripheral site might prevent Aβ peptide deposition induced by AChE. This enzyme has a narrow 20 Å deep active site gorge, the bottom and opening regions of which are known as catalytic and peripheral sites, respectively (Figure 1). AChE inhibitors simultaneously blocking both the catalytic and peripheral sites might not only alleviate the cognitive deficit of AD patients by elevating ACh levels but also act as disease-modifying agents delaying amyloid plaque formation.[9a,13]

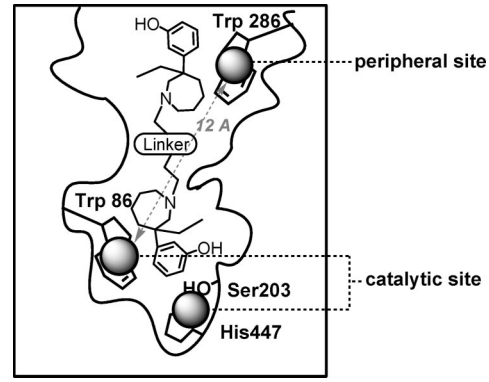

Figure 1. Catalytic and peripheral sites of AChE active site gorge.

Recently, bivalent ligand strategy has been utilized in the design of dual binding site AChE inhibitors.[9–13] Homobivalent or heterobivalent ligands are obtained by connecting two identical or distinct moieties through a linker of suitable length to make contact with both the catalytic and peripheral sites. A spatial 12 Å distance was determined by X-ray crystal diffraction from Trp86 (mammalian numbering), the catalytic anionic site center, to Trp286 (mammalian numbering), core of the peripheral site (Figure 1).[14] In many cases of homobivalent ligands (bis-ligands), AChE inhibitory potency and selectivity improved relative to the monomer and additional inhibition of AChE-induced Aβ aggregation was observed. Bis-tacrine **1** (Figure 2, n = 7)[9] was the first bivalent AChE inhibitor reported on this strategy, presenting a more than 1000-fold increase in AChE inhibiting potency and a 10000-fold increase in AChE/butyrylcholinesterase (BChE) selectivity compared with tacrine. Bis-galanthamine **2** (Figure 2, n = 8),[10] bis-5-amino-5,6,7,8-tetrahydroquinolinone **3** (Figure 2, n = 10 or 12),[11] and bis-

* To whom correspondence should be addressed. For Z.Q.: phone, 86-21-54237595; fax, 86-21-54237264; e-mail, zbqiu@shmu.edu.cn. For H.C.: phone, 86-21-63846590, extension 776450; fax, 86-21-64674721; e-mail, yaoli@shsmu.edu.cn.

† Fudan University.

# These authors contributed equally to this work.

‡ Shanghai JiaoTong University.

§ East China University of Science and Technology.

10.1021/jm070154q CCC: $40.75
Published on Web 03/12/2008

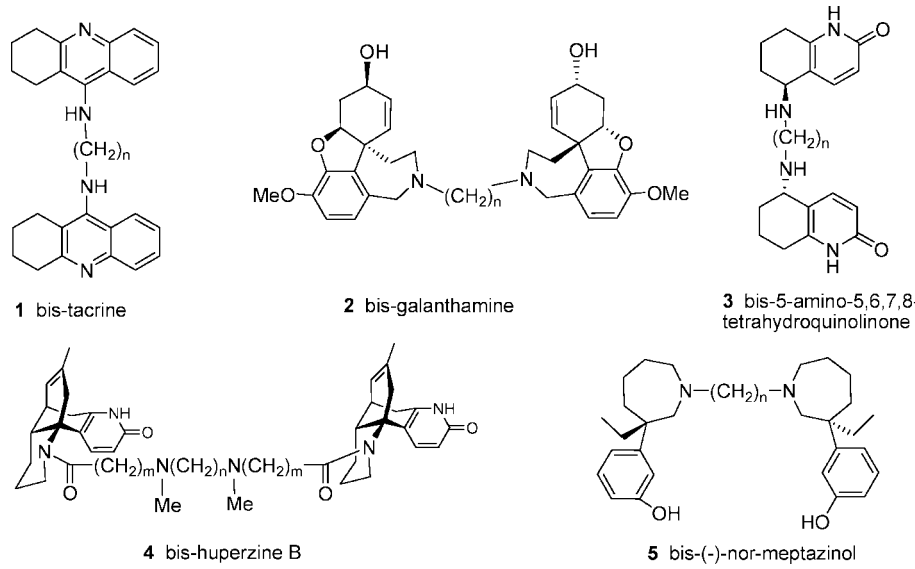

Figure 2. Structures of reported homobivalent AChE inhibitors and title compounds **5**.

Scheme 1. Synthesis of (−)-nor-MEP **8**[a]

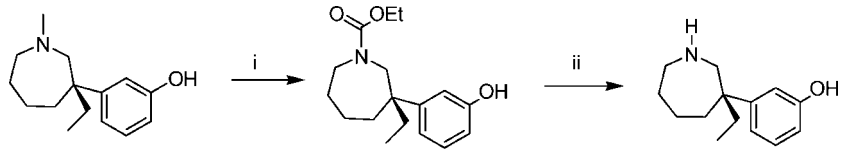

[a] Reagents and conditions: (i) (a) ClCOOEt, $KHCO_3$, $CHCl_3$, reflux, 1 h; (b) K_2CO_3 (aq), MeOH, N_2, room temp, 1 h, 95%; (ii) 50% H_2SO_4, N_2, reflux, 4 h, 54%.

huperzine B **4** (Figure 2, $m = 2$, $n = 10$)[12] (Figure 2) have also been reported.

Our group has been interested in the study of meptazinol (MEP),[15] a racemic marketed opioid analgesic with low addiction liability, and its (−)-enantiomer, which has demonstrated moderate inhibition of AChE.[16] We established an approach to the resolution of MEP in acceptable yields and determined the absolute configurations of (−)-MEP and (+)-MEP as *S* and *R*, respectively, by X-ray crystal structures.[17] Continuing with our previous research to find new AChE inhibitors through the molecular modeling of (−)-MEP derivatives,[18] we describe here the design, synthesis, pharmacological evaluation, and molecular docking of a series of homobivalent (−)-*N*-demethylmeptazinols (bis-(−)-nor-MEPs) **5**. Two identical (−)-nor-MEP units are connected by alkylene linkers of different lengths via the secondary amino groups in compound **5** (Figure 2).

A suitable length of the alkylene linker, together with an appropriate point of the coupling position, guarantees that bis-ligand will simultaneously bind to the catalytic and peripheral sites of the enzyme. According to our predicted binding mode of (−)-MEP in AChE active site,[18] the azepane ring is located in the middle of the gorge whereas the phenolic group is oriented down into the catalytic site at the bottom. Therefore, bivalent (−)-MEP derivatives were designed as bis-(−)-nor-MEPs linking, via a point in the azepane ring instead of the phenolic group (Figure 1). As to the chain length (number of methylene units), the optimal number in the case of tacrine-based bivalent ligands was 7.[9,19] However, that might not be the case in our study. To find the most potent compound in our series and discuss the effect of linker length on inhibitory potency, compounds possessing methylene spacers varying from 2 to 12 were synthesized.

Scheme 2. Synthesis of **5a**,**b**,**e**−**k**[a]

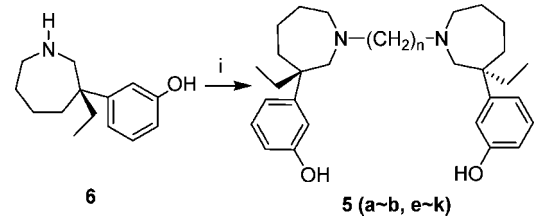

[a] Reagents and conditions: (i) α,ω-dihaloalkane (0.5 equiv), triethylamine (2 equiv), acetonitrile, reflux, 2−5 h, 35−83%.

Newly synthesized compounds were tested in vitro for AChE and BChE inhibitory potency, and their selectivity for AChE was calculated. A molecular docking study was performed on mouse AChE (mAChE) and human BChE (hBChE) to illuminate the binding modes of the most potent compound **5h** with both enzymes. Because of the unavailability of crystallographic data of mouse BChE, hBChE was used instead because of a high sequence identity. The ability of compounds **5g**, **5h**, and **5i** to inhibit the AChE-induced Aβ aggregation, compared with propidium iodine and the reference compound (−)-MEP, was assessed by means of a thioflavin T-based fluorometric assay.[20] Cell viability was tested by MTT assay for **5h** and **5i**.

Results and Discussion

Chemistry. The synthetic methodology employed for the preparation of bis-(−)-nor-MEP derivatives **5** is illustrated in Schemes 1−3. Key step in this route is the N-demethylation of (−)-MEP **6** producing (−)-nor-MEP **8**. A few methods have

Scheme 3. Synthesis of **5c**,**d**[a]

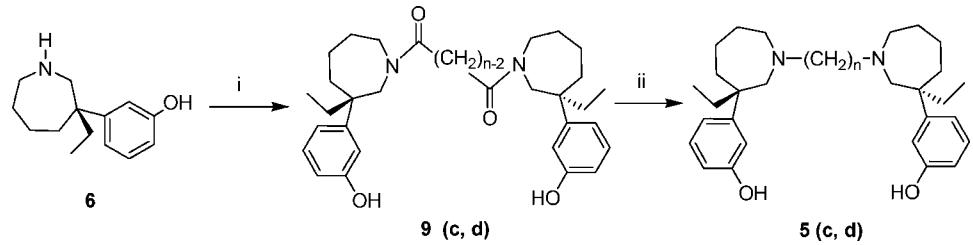

[a] Reagents and conditions: (i) α,ω-alkanediacyl dihalide (0.5 equiv), triethylamine (2 equiv), dry CH_2Cl_2, 0 °C, 15 min, 38−41%; (ii) lithium aluminum hydride (LAH), dry THF, reflux, 1 h, 31−36%.

been reported for the demethylation of tertiary amines, such as employment of azodicarboxylic acid esters,[21] cyanogen bromide,[22] or chloroformates.[23,24] Ethyl chloroformate was chosen as the reagent, taking both the availability and reaction simplicity into account. Treating (−)-MEP **6** with ethyl chloroformate in the presence of $KHCO_3$ in boiling $CHC1_3$, followed by dealing the resulting residue with a mild base, afforded a nonbasic carbamate intermediate, (−)-*N*-carboethoxy nor-MEP **7**. However, troubles were encountered in the hydrolysis and decarboxylation of the resulting carbamate intermediate **7**. All reactions failed under the reported alkaline condition in KOH[24] and acidic conditions in hydrobromic acid or 25% sulfuric acid. Finally this transformation was accomplished in 50% sulfuric acid under nitrogen for 4 h, and (−)-nor-MEP **8** was obtained in a 54% yield (Scheme 1).

Alkylation of (−)-nor-MEP **8** with α,ω-dihaloalkanes (0.5 equiv) in the presence of triethylamine, followed by chromatographic purification, easily produced the bis-(−)-nor-MEP compounds **5a**,**b**,**e**−**k** in 35−83% yield (Scheme 2). However, alkylation with 1,4-dichlorobutane or 1,5-dichloropentane failed to furnish the bivalent compounds **5c**,**d**, since the *N*-4-chlorobutyl (or 5-chloropentyl)-(−)-nor-MEP intermediate was prone to forming stable intramolecular five-membered or six-membered ring structures, resulting in failure to link another (−)-nor-MEP unit and leading to the generation of spiro quaternary ammoniums. Structures of two quaternary ammoniums derived from the *R* enantiomer were confirmed by X-ray crystallographic diffraction.[25] Eventually, the synthesis of the bis-ligands **5c**,**d** was accomplished by acylation with α,ω-alkanediacyl dihalide (0.5 equiv) to form bis-amides intermediates **9c**,**d** followed by reduction using lithium aluminum hydride (LAH) in tetrahydrofuran (THF) (Scheme 3).

The chemical structures of all target compounds or their synthesized hydrochloride salts were characterized by specific rotation $[\alpha]_D$, IR, ^{1}H NMR, and HR-ESI, as reported in the Experimental Section. The complicated property of NMR data from bis-(−)-nor-MEP hydrochloride salts in DMSO-d_6 resembled the case of (+)-MEP hydrochloride.[26] It was reasonably explained by conformational switch of the azepane ring and configurational inversion of nitrogen.

AChE Inhibitory Potency and AChE/BChE Selectivity. Newly synthesized compounds were tested in vitro for potency and selectivity as cholinesterase (ChE) inhibitors. Extracts from mice brain and mice serum were used as sources of AChE and BChE, respectively. The results showed that both (−)-MEP and its bis-ligand analogues possessed ChE inhibitory activity. The IC_{50} value of (−)-MEP was 41 μM, about 10 times higher than that obtained with AChE from bovine erythrocytes,[16] and the testing data of the reference drug rivastigmine conformed to the previous report.[27] The AChE inhibitory potency within the series of bis-(−)-nor-MEP derivatives was closely related to

Table 1. Inhibition of AChE and BChE by Bis-(−)-nor-MEPs **5a**−**k**, (−)-MEP, and Rivastigmine[a]

compd	chain length (*n*)	IC_{50} (nM) mice brain AChE	IC_{50} (nM) Mice serum BChE	selectivity for AChE[b]
5a	2	43000 ± 20000	125 ± 9	0.0029
5b	3	42000 ± 14000	132 ± 51	0.0031
5c	4	21400 ± 7600	104 ± 29	0.0049
5d	5	4000 ± 1000	192 ± 41	0.048
5e	6	1220 ± 20	119 ± 20	0.098
5f	7	270 ± 70	102 ± 19	0.38
5g	8	79 ± 19	63 ± 8	0.80
5 h	9	3.9 ± 1.3	10 ± 3	2.6
5i	10	9.5 ± 4.5	17 ± 6	1.8
5j	11	24 ± 8	74 ± 11	3.1
5k	12	42 ± 20	100 ± 55	2.4
rivastigmine		5500 ± 1500	1600 ± 30	0.29
(−)-MEP		41000 ± 14000	15000 ± 4000	0.37

[a] Mice brain homogenate prepared in normal saline was used as a source of AChE. Mice serum was the source of BChE. AChE was assayed spectrophotometrically with acetylthiocholine as substrate in the presence of 1024 M ethopropazine as BChE inhibitor. BChE was assayed similarly with butyrylthiocholine as substrate and 1025 M BW284C51 as AChE inhibitor. IC_{50} values were computed by a nonlinear least squares regression program that also provided an estimate of statistical precision (standard error of the mean). [b] Selectivity for AChE: IC_{50} for BChE divided by IC_{50} for AChE.

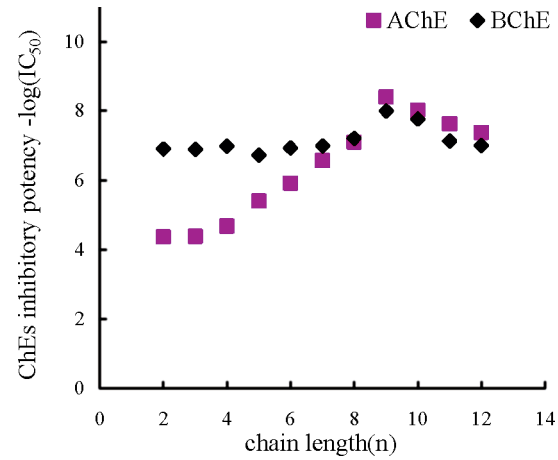

Figure 3. Correlation between ChE inhibitory potency (−log(IC_{50})) and the alkylene chain length (*n*) in compounds **5**.

the length of the alkylene chain. The optimal chain length determined experimentally was achieved in compound **5h**, with nine methylene groups between two (−)-nor-MEP units. Compared with (−)-MEP (IC_{50} = 41 μM) and rivastigmine (IC_{50} = 5.5 μM), **5h** (IC_{50} = 3.9 nM) showed a 10000-fold and 1400-fold increase, respectively, in the inhibition of mice brain AChE (Table 1). Further decrease or increase of the chain length weakened the AChE inhibition (Figure 3). For instance, the

inhibitory activities of **5a** and **5b** (43 and 42 μM, respectively) are similar to that of (−)-MEP. Therefore, the effective alkylene-bridged bis-(−)-nor-MEP analogues required chains of suitable length, which was 9 for the best, to bind at both the catalytic site and the peripheral site of the AChE binding pocket (gorge).

Compared with the AChE activity, the BChE inhibitory potency was less impacted by chain length (Figure 3). The majority of bis-(−)-MEP analogues showed inhibition on BChE of about 100 nM, although the highest potency (IC_{50} = 10 nM) was achieved in **5h**. This isomer was 1500 times and 150 times more potent than (−)-MEP (IC_{50} = 15 μM) and rivastigmine (IC_{50} = 1.6 μM), respectively, but only 10 times lower than that of the majority compounds (Table 1). The reason that the BChE inhibition is less sensitive to the linker length than the AChE inhibition seems to be the enzymic conformational difference. There is lack of a functional peripheral site in BChE,[28,29] and the BChE active site is wider throughout. Therefore, there is no restriction of linker length for bivalent BChE inhibitors.

Most bis-ligand analogues showed greater selectivity for BChE because of their low affinity for AChE. Only four compounds, **5h**, **5i**, **5j**, and **5k**, demonstrated slightly more selectivity for AChE. Recent evidence suggests that both AChE and BChE may play roles in the etiology and progression of AD beyond regulation of synaptic ACh levels. In the AD brain, the activity of AChE decreases progressively in certain regions to reach 10–15% of normal values, whereas the activity of BChE stays unchanged or is even increased by 20%.[30] Thus, it may not be an advantage for a ChE inhibitor to be considerably more selective for AChE; on the contrary, a good balance between AChE and BChE may result in higher efficacy. As a dual inhibitor of both AChE and BChE, rivastigmine appears to be beneficial for people with mild to moderate AD, and BChE inhibition correlates significantly with cognitive improvement in these patients.[31] In our study, although **5h** is slightly more selective for AChE than BChE (2.6), it had the greatest inhibition at a nanomolar lever on both enzymes. Therefore, it was suggested that it was a promising drug candidate worthy of further investigations.

Molecular Docking Studies. Molecular docking study was performed to ascertain the possibility for the most potent compound **5h** to bind at both the catalytic and peripheral sites of AChE and to explore the difference in the interactions of **5h** with AChE and BChE. Mammalian enzymes were used in docking, compatible with the pharmacological test. Because of the unavailability of crystallographic data of mouse BChE, hBChE was used instead because there is a high sequence identity (82%) especially between mouse and human BChE and the residues in active sites are highly conservative. Here, we chose recently resolved X-ray crystal structures of the mAChE complex with succinylcholine[32] with a high resolution of 2.05 Å and of native hBChE[28] with a 2.0 Å resolution. GOLD[33] docking protocol was employed because it has been proved by our previous study[18] to be accurate and reliable for reproducing the binding modes of seven AChE inhibitors in their X-ray crystal structures of *Torpedo californica* AChE (TcAChE) complexes. An advanced consensus scoring technology was used to guide the selection of the most reliable conformation from a set of candidate conformations that GOLD generated.

Our results show that **5h** is able to simultaneously make contact with both the catalytic and peripheral sites of mAChE, as illustrated in Figure 4a. The key interactions of these dimeric inhibitors with the catalytic and peripheral sites are π-stacking and cation−π interactions. The phenyl group of the nor-MEP buried within the core of the enzyme binds with the catalytic site via face-to-face π-stacking interaction with Trp86 (distance between the two centroids: 4.27 Å). The other nor-MEP moiety reaches the peripheral site on the surface of the enzyme by cation−π and hydrophobic interactions between the seven-membered azepane ring and Trp286 (distance between the two centroids: 4.09 Å). The spatial distance between the centroids of the centric phenyl group and the peripheral azepane ring is 13.5 Å, consistent with the reported distance between two tryptophanes.[14] **5h** forms two hydrogen bonds, both in the catalytic active site. The hydroxyl is hydrogen-bonded to the main-chain carbonyl oxygen of His447 (O···O distance: 2.87 Å). Meanwhile, the protonated azepane amino group is hydrogen-bonded to the hydroxyl oxygen of Tyr124 (N···O distance: 3.22 Å). In addition, other aliphatic and aromatic residues are involved in hydrophobic interactions, as shown in Figure 4b.

In comparison, the binding mode of **5h** with the active site of hBChE is shown in Figure 4c,d. **5h** is folded in the large cavity along the aliphatic residue-dominated wall, and the separation of two terminal (−)-nor-MEP units is relatively short. Three hydrogen bonds are found: (i) between the phenolic hydroxyl within the core of the enzyme and the carboxylic acid oxygen of Asp70 (O···O distance, 2.49 Å); (ii) between the phenolic hydroxyl at the entrance of the enzyme and the carboxylic acid oxygen of Glu276 (O···O distance, 2.61 Å); and (iii) between the oxygen on the phenolic hydroxyl at the entrance and the side chain amide NH of Gln119 (O···N distance, 3.22 Å). Ala 277 and Ala328 are not so importantly involved in the hydrophobic interactions with **5h**, unlike the way their counterparts Try286 and Tyr337 in the mAChE catalytic site behave. On the contrary, some residues unique to hBChE, such as Gln119, Leu286, and Val288, form hydrophobic contacts with **5h.**

The difference in the binding mode as well as in pharmacological activities between **5h** with AChE and BChE is fundamentally caused by conformational differences between the two enzymes. One of the most important differences is the lack of peripheral site in BChE. Residues responsible for $\pi-\pi$ or cation−π interactions at AChE peripheral site are replaced by aliphatic residues in BChE. For example, Trp286, Tyr72, and Tyr124 in mAChE are the counterparts of Ala277, Asn68, and Gln119 in hBChE, respectively. In addition, some bulky aromatic residues in AChE active site have been replaced by small aliphatic ones in BChE. As a result, the active site of BChE is wider and able to accommodate bis-ligands with linkers of wider-ranging lengths. These might be the main reasons that the BChE inhibition is less sensitive to the linker length.

Inhibition of AChE-Induced Aβ Aggregation. Three compounds, **5g**, **5h**, and **5i**, were selected to assess their abilities to inhibit Aβ aggregation induced by AChE using a thioflavin T-based fluorometric assay,[20] compared with the reference compound propidium iodine (Sigma-Aldrich), a known specific peripheral site-binding inhibitor, and the monomer (−)-MEP (Table 2). Results showed that **5h** and **5i** markedly prevented the AChE-induced Aβ aggregation with IC_{50} values of 16.6 and 5.8 μM, similar to that of propidium (IC_{50} = 12.8 μM). With a small IC_{50} value and a higher efficiency of inhibition, **5i** and **5h** were the wonderful compounds that inhibited the aggregation of Aβ induced by AChE. In contrast, (−)-MEP and **5g** showed fairly low inhibitory activity (Table 2), which indicated their limited ability to interact with the peripheral site of the enzyme.

Different behaviors of these four compounds were attributed to different lengths of linker, demonstrating that a linker no shorter than 9 was necessary to inhibit AChE-induced Aβ

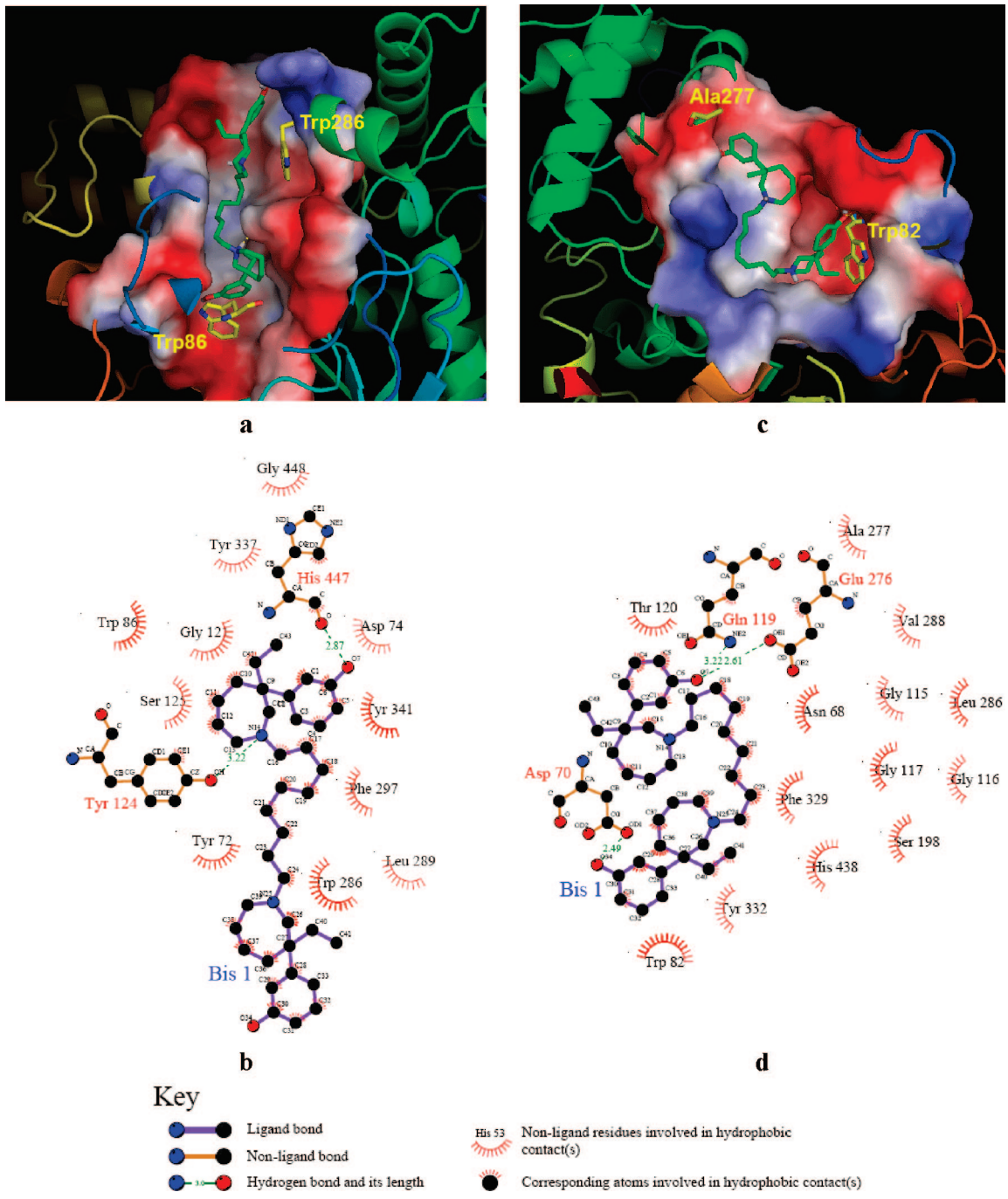

Figure 4. Representation of **5h** (C atoms colored green) docked into the binding sites of mAChE (a) and hBChE (c). The binding site surfaces are colored according to the vacuum electrostatics protein contact potential, calculated by PyMOL 0.99rc2 (DeLano Scientific LLC, San Carlos, CA). Crucial catalytic and peripheral site (or the counterpart) residues are colored yellow. Hydrogen bonds and hydrophobic contacts between **5h** and the protein residues of mAChE (b) and hBChE (d) are shown by LigPlot 4.4.2.[41]

aggregation. These findings agree with the results from enzymatic test and molecular docking, which indicated that a linker of 9 or 10 methylenes would help to reach the peripheral site of AChE.

Cell Viability. The toxicity of the most potent two bis-(−)-nor-MEPs was determined in human neuroblastoma cell line SH-SY5Y. Cell viability was not affected for **5h** and **5i** at concentrations of 1–100 μM (higher than the IC_{50} values of **5h** and **5i** against β-amyloid aggregation inhibition (around 80 μM) and 10000 times higher than their AChE inhibiting IC_{50} values).

Conclusion

We have discovered novel nanomolar ChE inhibitors with high inhibitory potency on Aβ aggregation, i.e., a series of bis-(−)-nor-MEPs **5**. Their AChE inhibitory activities were closely related to the length of the alkylene chain, whereas BChE inhibition was less influenced. The optimal chain length for AChE and BChE inhibition was achieved with 9 in **5h**, which showed a 10000-fold and 1500-fold increase in the inhibition of mice brain AChE and mice serum BChE, respectively, compared with (−)-MEP. Molecular docking elucidated that **5h** simultaneously bound to the catalytic and peripheral sites via hydrophobic interactions with Trp86 and Trp286 in mAChE. In comparison, it folded in the large aliphatic cavity of hBChE. The differences were explained by the absence of peripheral site and the enlargement of the active site gorge in BChE. Furthermore, **5h** and **5i** markedly prevented the AChE-induced

Table 2. Inhibition of AChE-Induced Aβ Aggregation by Bis-(−)-nor-MEPs **5g**−**i** and Reference Compounds

compd	chain length (n)	inhibition (%) at 100 μM	inhibition (%) at 200 μM	IC_{50} (μM)
propidium iodine		85.6 ± 4.4	98.6 ± 5.9	12.8 ± 0.4
(−)-MEP		nd[a]	0	nd[a]
5g	8	0	15.2 ± 0.2	nd[a]
5h	9	90.8 ± 0.2	99.2 ± 0.1	16.6 ± 0.5
5i	10	95.8 ± 0.5	98.4 ± 0.1	5.8 ± 0.3

[a] nd: not determined.

Aβ aggregation with IC_{50} values of 16.6 and 5.8 μM, compatible with that of propidium (IC_{50} = 12.8 μM), which pointed out a promising disease-modifying action. Further pharmacological study is needed to evaluate their abilities to reverse memory impairment in animal models in order to select ideal candidates for the treatment of AD patients.

Experimental Section

Chemistry. Melting points were taken in glass capillary tubes and were uncorrected. Specific rotation ($[\alpha]_D$) was determined on a JASCOP-1020 rotatory apparatus. IR data were taken on an AVATAR 360 FT-IR spectrometer (KBr). NMR data were recorded with a Mercury Plus 400 instrument. Chemical shifts (δ) are expressed in parts per million (ppm) relative to tetramethylsilane (TMS) as an internal standard. All signals of active hydrogen disappeared after D_2O exchange. Mass spectra were measured on an Agilent 1100 series LC/MSD 1946D spectrometer. HRMS spectra were recorded with an IonSpec 4.7 T FTMS instrument. The purity of all target compounds (>95%) was verified via HPLC. The elution was methanol−0.05 mol/L ammonium acetate solution (adjustment of pH to 7.4 with aqueous ammonia) (70:30 to 80:20). The chromatographic condition was a flow rate of 1.0 mL/min with UV detection at 225 nm on a VP-ODS C18 (150 mm × 4.6 mm, 5 μm) column at a temperature of 50 °C. All reagents were of commercial quality. Rivastigmine hydrochloride standard was available from Sunve (Shanghai) Pharmaceutical Co., Ltd.

(−)-*N*-Carboethoxy-nor-MEP (7). A stirred suspension of (−)-MEP **6** (9.83 g, 42.2 mmol) and $KHCO_3$ (74 g, 740 mmol) in boiling $CHCl_3$ (500 mL) was treated with ethyl chloroformate (30.5 mL, 320 mmol) and refluxed for 1 h. H_2O (350 mL) was added, and the $CHCl_3$ phase was separated and concentrated in vacuo. The residue was dissolved in MeOH (400 mL), treated with an aqueous solution (400 mL) containing 66 g of K_2CO_3, and stirred under N_2 at room temperature for 1 h. After the MeOH was removed, the residue was neutralized with 6 M HCl (126 mL) and extracted with Et_2O (150 mL × 3). The combined Et_2O extracts were washed with saturated NaCl solution (150 mL) and dried with anhydrous Na_2SO_4. Evaporation of the solvent under reduced pressure gave **7** (11.17 g, 95%) as a yellowish oil. Recrystallization of **7** (1.2 g) from ethyl acetate (2 mL) afforded **7** as off-white crystals (0.64 g, 53%): mp 79−81 °C; $[\alpha]_D$ −61.35° (*c* 0.11, MeOH); ^{1}H NMR ($CDCl_3$) 7.18 (t, H, *J* = 7.8 Hz, ArH), 6.87–6.81 (m, 2H, ArH), 6.70 (d, H, *J* = 8.0 Hz, ArH), 6.00 (br s, 1/2 H, Ar−OH), 5.57 (br s, 1/2 H, Ar−OH), 4.17–4.03 (m, 2H, $-OCH_2$), 3.94 (d, H, N−CH_2, *J* = 14.6 Hz), 3.90–3.85 (m, 1/2 H, N−$C\underline{H}_2CH_3$), 3.79–3.73 (m, 1/2 H, N−CH_2), 3.52 (d, 1/2H, *J* = 14.4 Hz, N−CH_2), 3.34 (d, 1/2 H, *J* = 14.9 Hz, N−CH_2), 3.06–2.95 (m, H, N−CH_2), 2.20–2.05 (m, H, CH_2), 1.77–1.58 (m, 7H, CH_2), 1.24 (m, 3H, $-OCH_2C\underline{H}_3$), 0.56 (t, 3H, *J* = 7.3 Hz, CH_3); MS (ESI) $[M + H]^+$ 292.2, $[M + Na]^+$ 314.2, $[M + K]^+$ 330.2.

(−)-Nor-MEP Hydrochloride (8·HCl). A mixture of **7** (11.17 g, 38.38 mmol) in 50% H_2SO_4 (120 mL) was refluxed under N_2 for 4 h. The solution was treated with aqueous ammonia (180 mL), adjusted to pH 9, and extracted with $CHCl_3$ (200 mL × 3). The combined $CHCl_3$ extracts were washed with saturated NaCl solution (200 mL) and dried with anhydrous Na_2SO_4. The solvent was removed in vacuo, and the oily residue underwent chromatography on a column of 170 g of silica gel (200−300 mesh) and gradient elution with EtOH/$CHCl_3$ (0.8:9.2 to 3:7). The eluent was concentrated in vacuo to afford **8** (4.58 g, 54%). Salt forming reaction of **8** (1.07 g) was carried out in dry ether by adding dry HCl−ether and adjusting the pH to 4, which afforded **8**·HCl as a white powder (0.98 g, 79%): mp 73−75 °C; $[\alpha]_D$ −7.10° (*c* 0.286, MeOH); IR ν 3257, 2932, 1614, 1588, 1481, 1432, 1321, 1276, 1237, 1211 cm^{-1}; ^{1}H NMR (DMSO-d_6) 9.42 (s, H, Ar−OH), 8.82 (br s, 1/2 H, NH^+), 8.24 (br s, 1/2 H, NH^+), 7.16 (t, H, *J* = 7.8 Hz, ArH), 6.74–6.65 (m, 3H, ArH), 3.49 (d, H, *J* = 14.1 Hz, N−CH_2), 3.21 (d, H, *J* = 14.5 Hz, N−CH_2), 3.08–3.00 (m, 2H, N−CH_2), 2.14 (m, H, CH_2), 1.77–1.55 (m, 7H, CH_2), 0.49 (t, 3H, *J* = 7.4 Hz, CH_3); MS (ESI) $[M + H]^+$ 220.1. HPLC: t_R = 1.86 min, 98.5% purity.

General Procedure for the Synthesis of Bis-(−)-Nor-MEP Compounds 5a,b,e−k. Triethylamine (2 equiv) and α,ω-dihaloalkane (0.5 equiv) were added to a solution of (−)-nor-MEP **8** in acetonitrile. The reaction mixture was refluxed for 2−5 h. Evaporation of the solvent gave a residue, which was diluted with saturated K_2CO_3 solution and extracted with $CHCl_3$. The combined $CHCl_3$ extracts were dried (anhydrous Na_2SO_4) and evaporated under reduced pressure. The residue was purified by chromatography on silica gel. Eluting with petroleum ether/EtOAc (1:2) afforded the corresponding bis-(−)-nor-MEP compounds **5** as a yellow oil. Addition of dry HCl−ether to a solution of **5** in dry ether and adjusting the pH to 3−4 gave the final salt **5**·2HCl as powder.

***N*,*N*′-(1′,2′-Ethylene)-bis-(−)-nor-MEP Hydrochloride (5a·2HCl).** (−)-nor-MEP **8** (1.50 g, 6.85 mmol), acetonitrile (15 mL), triethylamine (1.9 mL, 13.7 mmol), and 1,2-dibromoethane (0.297 mL, 3.43 mmol) were used to produce **5a** (0.80 g, 50%). Subsequent salt formation gave **5a**·2HCl (0.80 g, 86%): mp 142−145 °C; $[\alpha]_D$ −1.96° (*c* 0.204, MeOH); IR ν 3176, 2935, 1599, 1447, 1229 cm^{-1}; ^{1}H NMR (DMSO-d_6) 10.84 (br s, 1/2 H, NH^+), 10.58 (br s, H, NH^+), 9.51, 9.49, 9.43, 9.34(s, 2H, Ar−OH), 9.09 (br s, 1/2 H, NH^+), 7.22–7.08 (m, 2H, Ar−H), 6.83–6.61 (m, 6H, Ar−H), 3.79–3.71 (m, H, N−CH_2), 3.47–3.42 (m, H, N−CH_2), 3.14–3.10 (m, 2H, N−CH_2), 3.03–2.86 (m, 6H, N−CH_2), 2.71–2.69 (m, 2H, N−CH_2), 2.14–2.08 (m, 2H, CH_2), 1.84–1.46 (m, 14H, CH_2), 0.47 (m, 6H, CH_3); MS (ESI) $[M + H]^+$ 465.6. HRMS *m*/*z* calcd for $C_{30}H_{45}N_2O_2$ $[M + H]^+$, 465.3476; found, 465.3463. HPLC: t_R = 4.48 min, 98.2% purity.

***N*,*N*′-(1′,3′-Propylene)-bis-(−)-nor-MEP Hydrochloride (5b·2HCl).** (−)-nor-MEP **8** (1.54 g, 7.03 mmol), acetonitrile (15 mL), triethylamine (2.0 mL, 14.4 mmol), and 1,3-dibromopropane (0.357 mL, 3.52 mmol) were used to produce **5b** (1.20 g, 71%). Subsequent salt formation of **5b** (0.90 g) gave **5b**·2HCl (0.90 g, 87%): mp 165−168 °C; $[\alpha]_D$ −48.38° (*c* 0.228, MeOH); IR ν 3176, 2935, 1599, 1447, 1229 cm^{-1}; ^{1}H NMR (DMSO-d_6) 10.18, 9.97 (br s, 6/5 H, NH^+), 9.58, 9.52, 9.44, 9.42 (s, 2H, Ar−OH), 8.68, 8.59 (br s, 4/5 H, NH^+), 7.20–7.13 (m, 2H, Ar−H), 6.90–6.65 (m, 6H, Ar−H), 3.92 (d, 4/5 H, *J* = 14.5 Hz, N−CH_2), 3.56 (m, 6/5 H, N−CH_2), 3.44–3.21 (m, 10H, N−CH_2), 2.40 (m, 2H, CH_2), 2.10–1.50 (m, 16H, CH_2), 0.50 (m, 6H, CH_3); MS (ESI) $[M + H]^+$ 479.4, $[M + 2H]^{2+}$ 240.2. HRMS *m*/*z* calcd for $C_{31}H_{47}N_2O_2$ $[M + H]^+$, 479.3632; found, 479.3641. HPLC: t_R = 7.00 min, 99.1% purity.

***N*,*N*′-(1′,6′-Hexylene)-bis-(−)-nor-MEP Hydrochloride (5e·2HCl).** (−)-nor-MEP **8** (1.96 g, 8.95 mmol), acetonitrile (20 mL), triethylamine (2.5 mL, 18.0 mmol), and 1,6-dibromohexane (0.702 mL, 4.48 mmol) were used to produce **5e** (0.96 g, 41%). Subsequent salt formation gave **5e**·2HCl (1.06 g, 97%): mp 135−138 °C; $[\alpha]_D$ −47.8° (*c* 0.175, MeOH); IR ν 3414, 3176, 2938, 2876, 2732, 1600, 1585, 1447, 1269, 1232 cm^{-1}; ^{1}H NMR (DMSO-d_6) 10.05 (br s, 1/2 H, NH^+), 9.80 (br s, 3/4 H, NH^+), 9.56, 9.53, 9.44, 9.42 (s, 2H, Ar−OH), 8.43, 8.33 (br s, 3/4 H, NH^+), 7.22–7.13 (m, 2H, Ar−H), 6.87–6.76 (m, 4H, Ar−H), 6.71–6.66 (m, 2H, Ar−H), 3.84 (m, 3/4 H, N−CH_2), 3.55 (m, 5/4 H, N−CH_2), 3.34–3.09 (m, 10H, N−CH_2), 2.38 (m, H, CH_2), 2.12–1.73 (m, 15H, CH_2), 1.57–1.44 (m, 4H, CH_2), 1.35–1.25 (m, 4H, CH_2), 0.50 (t, 6H, *J* = 7.4 Hz, CH_3); MS (ESI) $[M + H]^+$ 521.7, $[M + 2H]^{2+}$ 261.4. HRMS *m*/*z* calcd for $C_{34}H_{53}N_2O_2$ $[M + H]^+$, 521.4102; found, 521.4086. HPLC: t_R = 8.10 min, 97.6% purity.

***N,N′*-(1′,7′-Heptylene)-bis-(−)-nor-MEP Hydrochloride (5f·2HCl).** (−)-nor-MEP **8** (1.70 g, 7.76 mmol), acetonitrile (20 mL), triethylamine (2.2 mL, 15.8 mmol), and 1,7-dibromoheptane (0.674 mL, 3.88 mmol) were used to produce **5f** (0.73 g, 35%). Subsequent salt formation gave **5f**·2HCl (0.70 g, 84%): mp 125−128 °C; $[\alpha]_D$ −44.29° (*c* 0.218, MeOH); IR *ν* 3417, 3186, 2938, 2866, 2740, 1600, 1585, 1447, 1268, 1232 cm^{-1}; ^1H NMR (DMSO-d_6) 9.70 (br s, 2/3 H, NH^+), 9.52, 9.50, 9.42, 9.41 (s, 2H, Ar−OH), 8.25 (br s, 4/3 H, NH^+), 7.22–7.14 (m, 2H, Ar−H), 6.87–6.66 (m, 6H, Ar−H), 3.85 (d, 4/5 H, *J* = 14.1 Hz, N−CH_2), 3.56 (d, 6/5 H, *J* = 14.1 Hz, N−CH_2), 3.39–3.01 (m, 10H, N−CH_2), 2.40 (m, 6/5 H, CH_2), 2.13 (m, 4/5 H, CH_2), 2.00–1.73 (m, 14H, CH_2), 1.53–1.45 (m, 4H, CH_2), 1.30 (m, 6H, CH_2), 0.50 (m, 6H, CH_3); MS (ESI) $[M + H]^+$ 535.8, $[M + 2H]^{2+}$ 268.4. HRMS *m/z* calcd for $C_{35}H_{55}N_2O_2$ $[M + H]^+$, 535.4258; found, 535.4258. HPLC: t_R = 9.67 min, 99.4% purity.

***N,N′*-(1′,8′-Octylene)-bis-(−)-nor-MEP Hydrochloride (5g·2HCl).** (−)-nor-MEP **8** (0.94 g, 4.29 mmol), acetonitrile (10 mL), triethylamine (1.2 mL, 8.63 mmol), and 1,8-dibromooctane (0.406 mL, 2.15 mmol) were used to produce **5g** (0.43 g, 37%). Subsequent salt formation of **5g** (0.31 g) gave **5g**·2HCl (0.29 g, 83%): mp 101−106 °C; $[\alpha]_D$ −37.8 ° (*c* 0.099, MeOH); IR *ν* 3420, 2936, 1600, 1447, 1269 cm^{-1}; ^1H NMR (DMSO-d_6) 10.11, 9.95 (br s, 4/3 H, NH^+), 9.57, 9.54, 9.45, 9.43 (s, 2H, Ar−OH), 8.43, 8.35 (br s, 2/3 H, NH^+), 7.19–7.11 (m, 2H, Ar−H), 6.85–6.64 (m, 6H, Ar−H), 3.81 (d, 2/3 H, *J* = 14.1 Hz, N−CH_2), 3.53 (d, 4/3 H, *J* = 13.7 Hz, N−CH_2), 3.35–3.28 (m, 3H, N−CH_2), 3.15–3.05 (m, 7H, N−CH_2), 2.38–2.33 (m, H, CH_2), 2.11–1.96 (m, 3H, CH_2), 1.80–1.70 (m, 12H, CH_2), 1.51–1.41 (m, 4H, CH_2), 1.28–1.24 (m, 8H, CH_2), 0.47 (t, 6H, *J* = 7.4 Hz, CH_3); MS (ESI) $[M + H]^+$ 549.4, $[M + 2H]^{2+}$ 275.2. HRMS *m/z* calcd for $C_{36}H_{57}N_2O_2$ $[M + H]^+$, 549.4415; found, 549.4428. HPLC: t_R = 12.25 min, 97.9% purity.

***N,N′*-(1′,9′-Nonylene)-bis-(−)-nor-MEP Hydrochloride (5h·2HCl).** (−)-nor-MEP **8** (0.89 g, 4.06 mmol), acetonitrile (10 mL), triethylamine (1.2 mL, 8.62 mmol), and 1,9-dibromononane (0.423 mL, 2.03 mmol) were used to produce **5h** (0.71 g, 62%). Subsequent salt formation of **5h** (0.67 g) gave **5h**·2HCl (0.62 g, 82%): mp 118−124 °C; $[\alpha]_D$ −39.13° (*c* 0.32, MeOH); IR *ν* 3423, 2934, 1600, 1585, 1446, 1268 cm^{-1}; ^1H NMR (DMSO-d_6) 10.10, 9.95 (br s, 4/3 H, NH^+), 9.56, 9.54, 9.44 (s, 2H, Ar−OH), 8.41, 8.34 (br s, 2/3 H, NH^+), 7.19–7.11 (m, 2H, Ar−H), 6.84–6.64 (m, 6H, Ar−H), 3.82 (d, 2/3 H, *J* = 14.1 Hz, N−CH_2), 3.53 (d, 4/3 H, *J* = 13.7 Hz, N−CH_2), 3.38–3.27 (m, 3H, N−CH_2), 3.15–3.04 (m, 7H, N−CH_2), 2.38–2.32 (m, H, CH_2), 2.10–2.01 (m, 3H, CH_2), 1.79–1.70 (m, 12H, CH_2), 1.54–1.41 (m, 4H, CH_2), 1.29–1.27 (m, 10H, CH_2), 0.47 (t, 6H, *J* = 7.4 Hz, CH_3); MS (ESI) $[M + H]^+$ 563.5, $[M + 2H]^{2+}$ 282.3. HRMS *m/z* calcd for $C_{37}H_{59}N_2O_2$ $[M + H]^+$, 563.4571; found, 563.4553. HPLC: t_R = 15.98 min, 98.4% purity.

***N,N′*-(1′,10′-Decylene)-bis-(−)-nor-MEP Hydrochloride (5i·2HCl).** (−)-nor-MEP **8** (0.83 g, 3.78 mmol), acetonitrile (10 mL), triethylamine (1.1 mL, 7.91 mmol), and 1,10-dibromodecane (0.438 mL, 1.89 mmol) were used to produce **5i** (0.51 g, 47%). Subsequent salt formation of **5i** (0.47 g) gave **5i**·2HCl (0.45 g, 85%): mp 104−108 °C; $[\alpha]_D$ −38.43° (*c* 0.27, MeOH); IR *ν* 3417, 3176, 2932, 2856, 2733, 1600, 1585, 1447, 1269, 1230 cm^{-1}; ^1H NMR (DMSO-d_6) 10.09, 9.94 (br s, 4/3 H, NH^+), 9.57, 9.54, 9.46, 9.45 (s, 2H, Ar−OH), 8.41, 8.34 (br s, 2/3H, NH^+), 7.18–7.11 (m, 2H, Ar−H), 6.84–6.64 (m, 6H, Ar−H), 3.82 (d, 2/3 H, *J* = 14.5 Hz, N−CH_2), 3.52 (d, 4/3 H, *J* = 14.1 Hz, N−CH_2), 3.36–3.27 (m, 3H, N−CH_2), 3.14–3.03 (m, 7H, N−CH_2), 2.38–2.32 (m, H, CH_2), 2.13–1.95 (m, 3H, CH_2), 1.79–1.70 (m, 12H, CH_2), 1.54–1.41 (m, 4H, CH_2), 1.28–1.25 (m, 12H, CH_2), 0.47 (t, 6H, *J* = 7.0 Hz, CH_3); MS (ESI) $[M + H]^+$ 577.5, $[M + 2H]^{2+}$ 289.3. HRMS *m/z* calcd for $C_{38}H_{61}N_2O_2$ $[M + H]^+$, 577.4728; found, 577.4747. HPLC: t_R = 22.13 min, 98.9% purity.

***N,N′*-(1′,11′-Undecydene)-bis-(−)-nor-MEP Hydrochloride (5j·2HCl).** (−)-nor-MEP **8** (0.78 g, 3.56 mmol), acetonitrile (10 mL), triethylamine (1.0 mL, 7.20 mmol), and 1,11-dibromoundecane (0.418 mL, 1.78 mmol) were used to produce **5j** (0.50 g, 48%). Subsequent salt formation gave **5j**·2HCl (0.47 g, 84%): mp 108−112 °C; $[\alpha]_D$ −38.53° (*c* 0.29, MeOH); IR *ν* 3423, 3180, 2927, 2856, 1600, 1585, 1446, 1267, 1232 cm^{-1}; ^1H NMR (DMSO-d_6) 10.13, 10.02 (br s, 7/5 H, NH^+), 9.58, 9.55, 9.47, 9.45 (s, 2H, Ar−OH), 8.41, 8.37 (br s, 3/5 H, NH^+), 7.18–7.10 (m, 2H, Ar−H), 6.84–6.64 (m, 6H, Ar−H), 3.81 (d, 3/5 H, *J* = 14.1 Hz, N−CH_2), 3.52 (d, 7/5 H, *J* = 13.7 Hz, N−CH_2), 3.42–3.26 (m, 3H, N−CH_2), 3.14–3.03 (m, 7H, N−CH_2), 2.37–2.32 (m, H, CH_2), 2.10–1.97 (m, 3H, CH_2), 1.82–1.70 (m, 12H, CH_2), 1.54–1.37 (m, 4H, CH_2), 1.27–1.24(m, 14H, CH_2), 0.47 (t, 6H, *J* = 7.4 Hz, CH_3); MS (ESI) $[M + H]^+$ 591.3. HRMS *m/z* calcd for $C_{39}H_{63}N_2O_2$ $[M + H]^+$, 591.4884; found, 591.4901. HPLC: t_R = 15.30 min, 98.9% purity.

***N,N′*-(1′,12′-Dodecydene)-bis-(−)-nor-MEP Hydrochloride (5k·2HCl).** (−)-nor-MEP **8** (0.69 g, 3.15 mmol), acetonitrile (10 mL), triethylamine (0.9 mL, 6.47 mmol), and 1,12-dibromododecane (0.53 mL, 1.58 mmol) were used to produce **5k** (0.34 g, 36%). Salt formation of **5k** (0.58 g) gave **5k**·2HCl (0.49 g, 80%): mp 100−105 °C; $[\alpha]_D$ −35.77° (*c* 0.30, MeOH); IR *ν* 3419, 2927, 2855, 1600, 1585, 1446, 1269; ^1H NMR (DMSO-d_6) 10.00 (br s, 4/3 H, NH^+), 9.49, 9.48, 9.40 (s, 2H, Ar−OH), 8.23 (br s, 2/3 H, NH^+), 7.19–7.11 (m, 2H, Ar−H), 6.85–6.64 (m, 6H, Ar−H), 3.82 (d, 4/5 H, *J* = 13.7 Hz, N−CH_2), 3.53 (d, 6/5 H, *J* = 13.3 Hz, N−CH_2), 3.37–3.30 (m, 3H, N−CH_2), 3.15–3.05 (m, 7H, N−CH_2), 2.36–2.31 (m, H, CH_2), 2.10 (m, H, CH_2), 1.81–1.70 (m, 14H, CH_2), 1.52–1.42 (m, 4H, CH_2), 1.27–1.24 (m, 16H, CH_2), 0.48 (m, 6H, CH_3); MS (ESI) $[M + H]^+$ 605.3. HRMS *m/z* calcd for $C_{40}H_{65}N_2O_2$ $[M + H]^+$, 605.5041; found, 605.5054. HPLC: t_R = 19.73 min, 96.1% purity.

General Procedure for the Synthesis of Intermediate Amide Compounds 9c,d. Triethylamine (2 equiv) was added to a solution of (−)-nor-MEP **8** in dry CH_2Cl_2. Then α,ω-alkanediacyl dihalide (0.5 equiv) in dry CH_2Cl_2 was added dropwise at 0 °C. The mixture was stirred for 15 min at 0 °C. The mixture was washed with H_2O (5 mL), 2 M HCl (8 mL), and then H_2O (5 mL). The combined water layers were back-extracted with CH_2Cl_2 (10 mL × 3). All the CH_2Cl_2 layers were combined and dried with anhydrous Na_2SO_4. Evaporation of the solvent under reduced pressure gave a yellowish foam. Purification by chromatography on silica gel eluted with petroleum ether/EtOAc (1:3) afforded the amide intermediates **9c**,**d** as a white foam.

***N,N′*-(1′,4′-Succinyl)-bis-(−)-nor-MEP (9c).** (−)-nor-MEP **8** (1.45 g, 6.63 mmol), CH_2Cl_2 (35 mL), triethylamine (1.84 mL, 12.2 mmol), and succinyl chloride (0.382 mL, 3.30 mmol) were used to produce **9c** (0.73 g, 41%). IR *ν* 3170, 2966, 2936, 1737, 1614, 1596, 1455, 1427, 1266, 1238, 1202 cm^{-1}; ^1H NMR (DMSO-d_6) 8.79 (s, 2H, Ar−OH), 7.19 (t, 2H, Ar−H), 6.78–6.70 (m, 6H, Ar−H), 4.88 (d, 2H, *J* = 14.7 Hz, N−CH_2), 3.59 (dd, 2H, J_1 = 11.7 Hz, J_2 = 7.0 Hz, N−CH_2), 3.08 (d, 2H, *J* = 15.0 Hz, N−CH_2), 2.91 (t, 2H, *J* = 11.7 Hz, CH_2), 2.83 (d, 2H, *J* = 13.6 Hz, N−CH_2), 2.39 (dm, 2H, *J* = 7.7 Hz, N−CH_2), 2.33 (d, 2H, *J* = 13.2 Hz, N−CH_2), 1.82–1.48 (m, 14H, CH_2), 0.68 (t, 6H, *J* = 7.3 Hz, CH_3); MS (ESI) $[M + H]^+$ 521.3.

***N,N′*-(1′,5′-Glutaryl)-bis-(−)-nor-MEP (9d).** (−)-nor-MEP **8** (1.59 g, 7.26 mmol), CH_2Cl_2 (35 mL), triethylamine (2.02 mL, 14.4 mmol), and glutaryl chloride (0.481 mL, 3.63 mmol) were used to produce **9d** (0.74 g, 38%). IR *ν* 3383, 2933, 2877, 1616, 1583, 1443, 1264 cm^{-1}; ^1H NMR ($CDCl_3$) 8.54, 8.10, 7.77, 7.52 (brs × 4, 2H, Ar−OH), 7.17 (t, 2H, Ar−H), 7.05–6.93 (m, 2H, Ar−H), 6.82–6.70 (m, 4H, Ar−H), 4.53 (d, H, *J* = 14.9 Hz, N−CH_2), 3.75–3.49 (m, 3H, N−CH_2), 3.41–3.18 (m, 2H, N−CH_2), 2.99–2.94 (m, H, N−CH_2), 2.54–2.46 (m, H, N−CH_2), 2.34–2.17 (m, 4H, CO−CH_2), 1.93–1.50 (m, 18H, CH_2), 0.62–0.51 (m, 6H, CH_3); MS (ESI) $[M + H]^+$ 535.3.

General Procedure for the Synthesis of Bis-(−)-nor-MEP Compounds 5c,d. A solution of **9c**,**d** in dry THF was added dropwise to lithium aluminum hydride (5 equiv) in dry THF at room temperature. The mixture was refluxed for 1 h, and then H_2O, 15% NaOH, and H_2O were added. The mixture was stirred for 15 min at room temperature. The mixture was filtered, and the solid material was washed with THF. The combined THF solution was evaporated to remove solvents. The residue was treated with H_2O

(15 mL), drops of aqueous ammonia were added to adjust the pH to 9, and the residue was extracted with $CHCl_3$ (20 mL × 3). The combined $CHCl_3$ was dried with anhydrous Na_2SO_4 and concentrated in vacuo to give a residue, which was chromatographed on silica gel and eluted with MeOH/$CHCl_3$ (0.5:9.5) to provide **5c**,**d** as an oil. Addition of dry HCl−ether to the solution of **5c**,**d** in dry ether, with pH adjusted to 3−4, gave the final salt **5c**,**d**·2HCl as a powder.

***N*,*N*′-(1′,4′-Butylene)-bis-(−)-nor-MEP Hydrochloride (5c·2HCl).** Compound **9c** (0.56 g, 1.08 mmol), lithium aluminum hydride (0.20 g, 5.26 mmol), THF (30 mL), H_2O (0.20 mL), 15% NaOH (0.20 mL), and H_2O (0.60 mL) were used to produce **5c** (0.19 g, 36%). Subsequent salt formation gave **5c**·2HCl (0.12 g, 55%): mp 110−115 °C; $[\alpha]_D$ −51.96° (*c* 0.092, MeOH); IR *ν* 3254, 2936, 1600, 1586, 1448, 1268 cm^{-1}; ^1H NMR (DMSO-d_6) 9.98, 9.77 (br s, 4/3 H, NH^+), 9.56, 9.54, 9.43, 9.42 (s, 2H, Ar−OH), 8.46 (br s, 2/3 H, NH^+), 7.21–7.13 (m, 2H, Ar−H), 6.85–6.65 (m, 6H, Ar−H), 3.83 (m, ∼2/3 H, N−CH_2), 3.52 (m, ∼4/3 H, N−CH_2), 3.36–3.15 (m, 10H, N−CH_2), 2.38 (m, H, CH_2), 2.10–1.46 (m, 19H, CH_2), 0.49 (t, 6H, J = 7.0 Hz, CH_3); MS (ESI) $[M + H]^+$ 493.3, $[M + 2H]^{2+}$ 247.2. HRMS *m*/*z* calcd for $C_{32}H_{49}N_2O_2$ $[M + H]^+$, 493.3791; found, 493.3789. HPLC: t_R = 7.45 min, 98.0% purity.

***N*,*N*′-(1′,5′-Pentylene)-bis-(−)-nor-MEP Hydrochloride (5d·2HCl).** Compound **9d** (0.55 g, 1.03 mmol), lithium aluminum hydride (0.20 g, 5.26 mmol), THF (30 mL), H_2O (0.20 mL), 15% NaOH (0.20 mL), and H_2O (0.60 mL) were used to produce **5d** (0.16 g, 31%). Subsequent salt formation of **5d** (0.10 g) gave **5d**·2HCl (0.06 g, 52%): mp 80−82 °C; $[\alpha]_D$ −48.10° (*c* 0.084, MeOH); IR *ν* 3417, 2937, 1600, 1585, 1447, 1268 cm^{-1}; ^1H NMR (DMSO-d_6) 9.96, 9.75 (br s, 5/4 H, NH^+), 9.57, 9.52, 9.44, 9.42 (s, 2H, Ar−OH), 8.34 (br s, 3/4 H, NH^+), 7.19–7.12 (m, 2H, Ar−H), 6.83–6.64 (m, 6H, Ar−H), 3.82 (m, 3/4 H, N−CH_2), 3.52 (m, 5/4 H, N−CH_2), 3.34–3.06 (m, 10H, N−CH_2), 2.37 (m, H, CH_2), 2.10–1.21 (m, 21H, CH_2), 0.48 (m, 6H, CH_3); MS (ESI) $[M + H]^+$ 507.3, $[M + 2H]^{2+}$ 254.2. HRMS *m*/*z* calcd for $C_{33}H_{51}N_2O_2$ $[M + H]^+$, 507.3945; found, 507.3961. HPLC: t_R = 7.77 min, 96.1% purity.

In Vitro AChE/BChE Inhibition Assay. Inhibitory activity against AChE was evaluated by a modified Ellman's method.[34] Mice brain homogenate prepared in saline was used as a source of AChE; mice serum was the source of BChE. The AChE activity was determined in a reaction mixture containing 200 μL of a solution of AChE (0.415 U/mL in 0.1 M phosphate buffer, pH 8.0), 300 μL of a solution of 5,5′-dithio-bis(2-nitrobenzoic) acid (3.3 mM DTNB in 0.1 M phosphate buffered solution, pH 7.0, containing $NaHCO_3$ 6 mM), and 30 μL of a solution of the inhibitor (six to seven concentrations). After incubation for 20 min at 37 °C, acetylthiocholine iodide (300 μL of 0.05 mM water solution) was added as the substrate, and AChE activity was determined by UV spectrophotometry from the absorbance changes at 412 nm for 3 min at 25 °C. The concentration of compound that produced 50% inhibition of the AChE activity (IC_{50}) was calculated by nonlinear regression of the response−concentration (log) curve. BChE inhibitory activity determinations were similarly carried out using butyrylthiocholine iodide (0.05 mM) as the substrate. Results are reported as the mean ± SEM of IC_{50} obtained from at least three independent measures.

Molecular Docking. Molecular simulations were performed on an R14000 SGI Fuel workstation with software package SYBYL 6.9 (Tripos Inc., St. Louis, MO). Standard parameters were used unless otherwise indicated. The X-ray crystallographic structures of the mAChE complex with succinylcholine (PDB code 2HA2)[32] and the native hBChE (1P0I)[28]were retrieved from PDB. Heteroatoms and water molecules in the PDB files were removed, and all hydrogen atoms were subsequently added to the protein. 3D coordinates of the ligand were generated by CORINA 3.0 (Molecular Networks GmbH, Erlangen, Germany, 2004).[35] Two sp^3 N atoms were both protonated, and the Gasteiger−Huckel partial charges[36,37] were assigned to each atom of the resultant ligand. The final conformation of the ligand was obtained after 1000 steps of energy minimization using the Tripos force field.

Molecular docking was carried out using GOLD 3.0 (CCDC, Cambridge, U.K., 2005)[33] to generate an ensemble of docked conformations for the ligand. The active site was defined as all atoms within a radius of 25 Å around some specific residue atoms: OH of Tyr337 for mAChE and $N^{\epsilon 2}$ of His438 for hBChE. We chose more enlarged binding pockets here, concerned that smaller sites might neither accommodate a large bis-ligand nor include both the catalytic and peripheral sites of AChE. The 600 genetic algorithm (GA) runs instead of the default 10 were performed owing to the high flexibility of the ligand possessing a great many rotatable bonds. For each GA run, the default GA settings were used except for the prohibited early termination and the permitted pyramidal nitrogen inversion.

Advanced combination approach of clustering and consensus scoring was used to guide the selection of the most reliable conformation from among a set of candidate conformations that GOLD generated. All conformations were evaluated with four available scoring functions, including three scoring functions (G_Score, D_Score, and ChemScore) from the CSCORE[38] module in SYBYL and another stand-alone scoring function, X-SCORE 1.2.1.[39] The "rank-by-rank" strategy reported by Wang et al.[40] was adopted to make consensus scoring. The final rank of a certain conformation was its average rank received from all four scoring functions. GOLD generated clusters based on different rmsd (root mean square deviation) criteria. A proper rmsd standard of clustering was important to the selection of representative clusters. Herein, rmsd values of 2.55 and 2.40 Å were chosen as the criteria to cluster the docked conformations with mAChE and hBChE, respectively. Among the top 10 clusters for each ChE, the one with members possessing the minimum average "rerank" was identified as the representative cluster. The top "reranked" conformation in the representative cluster was selected as the representative binding mode for the ligand.

Inhibition of AChE-Induced A*β* Aggregation. Aliquots of 2 μL A*β* (1–40) peptide (Biosource), lyophilized from 2 mg/mL HFIP solution and dissolved in DMSO, were incubated for 48 h at room temperature in 0.215 M sodium phosphate buffer (pH 8.0) at a final concentration of 230 μM. For coincubation experiments, aliquots (16 μL) of human recombinant AChE (Sigma-Aldrich) (final concentration of 2.3 μM, A*β*/AChE molar ratio of 100:1) and AChE in the presence of 2 μL of the tested inhibitors were added. Blanks containing A*β*, AChE, and A*β* plus inhibitors at various concentrations in 0.215 M sodium phosphate buffer (pH 8.0) were prepared. The final volume of each vial was 20 μL. Each assay was run in duplicate. Inhibitor stock solutions were prepared (c = 10 mM) and diluted in 0.215 M sodium phosphate buffer (pH 8.0) when used. To quantify amyloid fibril formation, the thioflavin T fluorescence method was then applied.[20]

After incubation, the samples containing A*β*, A*β* plus AChE, or A*β* plus AChE in the presence of inhibitors were diluted with 50 mM glycine−NaOH buffer (pH 8.5) containing 1.5 μM thioflavin T (Sigma-Aldrich) to a final volume of 2.0 mL. Fluorescence was monitored by PE LS45, with excitation at 446 nm and emission at 490 nm. A time scan of fluorescence was performed, and the intensity values reached at the plateau (around 300 s) were averaged after subtracting the background fluorescence from 1.5 μM thioflavin T and AChE. The percent inhibition of the AChE-induced aggregation due to the presence of increasing concentrations of the inhibitor was calculated by the following expression: 100 − (IF_i/IF_o × 100), where IF_i and IF_o were the fluorescence intensities obtained for A*β* plus AChE in the presence and in the absence of inhibitor, respectively, after subtracting the fluorescence of respective blanks. Inhibition curves and linear regression parameters were obtained for each compound, and the IC_{50} was extrapolated, when possible.

MTT Assay of Cell Viability. The human neuroblastoma cell line SH-SY5Y (American Type Culture Collection) cells were cultured in MEM/F-12 (1:1) medium (Invitrogen, Grand Island, NY) supplemented with 10% fetal calf serum (FCS, Invitrogen),

100 U/mL penicillin, and 100 μg/mL streptomycin in a humidified atmosphere containing 5% CO_2 at 37 °C. Cells were plated at 5×10^4 cells/well (200 μl) into 96-well plates and allowed to adhere and grow. When cells reached the required confluence, they were placed into serum-free medium and treated with the synthesized compounds **5h** and **5i**. Twenty-four hours later the survival of cells was determined by MTT assay. Briefly, after incubation with 20 μL of MTT (5 mg/mL; Sigma, St. Louis, MO) at 37 °C for 3 h, living cells containing MTT formazon crystals were solubilized in 200 μL of dimethyl sulfoxide (DMSO, Sigma). The absorbance of each well was measured using a microculture plate reader with a test wavelength of 570 nm and a reference wavelength of 655 nm.

Acknowledgment. We thank the National Natural Science Foundation of China (Grants 30472088, 30772553, and 30371731), the Program of Shanghai Subject Chief Scientist (Grant 06XD14011), and the Major Basic Research Project of Shanghai Municipal Science and Technology Commission (Grant 07DJ14005) for financial support. We also gratefully thank Dr. Manuela Bartolini (University of Bologna, Italy) and Dr. Margarita Dinamarca (Pontificia Universidad Católica, Chile) for their valuable suggestions in the experiments on AChE-induced Aβ aggregation.

Note Added after ASAP Publication. This manuscript was released ASAP on March 12, 2008 with errors in the Experimental and Acknowledgment Sections. The correct version posted on March 15, 2008.

References

(1) Walsh, D. M.; Selkoe, D. J. Deciphering the molecular basis of memory failure in Alzheimer's disease. *Neuron* **2004**, *44*, 181–193.
(2) Dekosky, S. T. Pathology and pathways of Alzheimer's disease with an update on new developments in treatment. *J. Am. Geriatr. Soc.* **2003**, *51*, 314–320.
(3) Bartus, R. T.; Dean, R. L.; Beer, B.; Lippa, A. S. The cholinergic hypothesis of geriatric memory dysfunction. *Science* **1982**, *217*, 408–414.
(4) Soreq, H.; Seidman, S. Acetylcholinesterases—new roles for an old actor. *Nat. Rev. Neurosci.* **2001**, *2*, 294–302.
(5) Alvarez, A.; Bronfman, F.; Pérez, C. A.; Vicente, M.; Garrido, J.; Inestrosa, N. C. Acetylcholinesterase, a senile plaque component, affects the fibrillogenesis of amyloid-beta-peptides. *Neurosci. Lett.* **1995**, *201*, 49–52.
(6) Alvarez, A.; Opazo, C.; Alarcón, R.; Garrido, J.; Inestrosa, N. C. Acetylcholinesterase promotes the aggregation of amyloid-β-peptide fragments by forming a complex with the growing fibrils. *J. Mol. Biol.* **1997**, *272*, 348–361.
(7) De Ferrari, G. V.; Canales, M. A.; Shin, I.; Weiner, L. M.; Silman, I.; Inestrosa, N. C. A structural motif of acetylcholinesterase that promotes amyloid beta-peptide fibril formation. *Biochemistry* **2001**, *40*, 10447–10457.
(8) Inestrosa, N. C.; Alvarez, A.; Pérez, C. A.; Moreno, R. D.; Vicente, M.; Linker, C.; Casanueva, O. I.; Soto, C.; Garrido, J. Acetylcholinesterase accelerates assembly of amyloid-β-peptides into Alzheimer's fibrils: possible role of the peripheral site of the enzyme. *Neuron* **1996**, *16*, 881–891.
(9) (a) Pang, Y. P.; Quiram, P.; Jelacic, T.; Hong, F.; Brimijoin, S. Highly potent, selective and low cost bis-tetrahydroaminacrine inhibitors of acetylcholinesterase: steps toward novel drugs for treating Alzheimer's disease. *J. Biol. Chem.* **1996**, *271*, 23646–23649. (b) Carlier, P. R.; Han, Y. F.; Chow, E. S. H.; Li, C. P. L.; Wang, H.; Lieu, T. X.; Wong, H. S.; Pang, Y. P. Evaluation of short-tether bis-THA AChE inhibitors. A further test of the dual binding site hypothesis. *Bioorg. Med. Chem.* **1999**, *7*, 351–357. (c) Rydberg, E. H.; Brumshtein, B.; Greenblatt, H. M.; Wong, D. M.; Shaya, D.; Williams, L. D.; Carlier, P. R.; Pang, Y. P.; Silman, I.; Sussman, J. L. Complexes of alkylene-linked tacrine dimers with *Torpedo californica* acetylcholinesterase: binding of bis(5)-tacrine produces a dramatic rearrangement in the active-site gorge. *J. Med. Chem.* **2006**, *49*, 5491–5500.
(10) (a) Mary, A.; Renko, D. Z.; Guillou, C.; Thal, C. Potent acetylcholinesterase inhibitors: design, synthesis, and structure−activity relationships of bis-interacting ligands in the galanthamine series. *Bioorg. Med. Chem.* **1998**, *6*, 1835–1850. (b) Guillou, C.; Mary, A.; Renko, D. Z.; Gras, E.; Thal, C. Potent acetylcholinesterase inhibitors: design, synthesis and structure−activity relationships of alkylene linked bis-galanthamine and galanthamine−galanthaminium salts. *Bioorg. Med. Chem. Lett.* **2000**, *10*, 637–639.
(11) Carlier, P. R.; Du, D. M.; Han, Y. F.; Liu, J.; Perola, E.; Williams, I. D.; Pang, Y. P. Dimerization of an inactive fragment of huperzine A produce a drug with twice the potency of the natural product. *Angew. Chem., Int. Ed.* **2000**, *39*, 1775–1777.
(12) Feng, S.; Wang, Z.; He, X.; Zheng, S.; Xia, Y.; Jiang, H.; Tang, X.; Bai, D. Bis-huperzine B: highly potent and selective acetylcholinesterase inhibitors. *J. Med. Chem.* **2005**, *48*, 655–657.
(13) Munoz-Torrero, D.; Camps, P. Dimeric and hybrid anti-Alzheimer drug candidates. *Curr. Med. Chem.* **2006**, *13*, 399–422.
(14) Harel, M.; Schalk, I.; Ehret-Sabatier, L.; Bouet, F.; Goeldner, M.; Hirth, C.; Axelsen, P. H.; Silman, I.; Sussman, J. L. Quaternary ligand binding to aromatic residues in the active-site gorge of acetylcholinesterase. *Proc. Natl. Acad. Sci. U.S.A.* **1993**, *90*, 9031–9035.
(15) Li, W.; Hao, J.; Tang, Y.; Chen, Y.; Qiu, Z. Comparative studies of X-ray determined meptazinol enantiomers with analgesic pharmacophore. *Acta. Pharmacol. Sin.* **2005**, *26*, 334–338.
(16) Ennis, C.; Haroun, F.; and Lattimer, N. Can the effects of meptazinol on the guinea-pig isolated ileum be explained by inhibition of acetylcholinesterase? *J. Pharm. Pharmacol.* **1986**, *38*, 24–27.
(17) Chen, Y. Studies on the Synthesis, Resolution and Optical Isomers of Meptazinol. Ph.D. Dissertation, Fudan University, Shanghai, P. R. China, 2004.
(18) Xie, Q.; Tang, Yun.; Li, W.; Wang, X.; Qiu, Z. Investigation of the binding mode of (−)-meptazinol and bis-meptazinol derivatives on acetylcholinesterase using a molecular docking method. *J. Mol. Model.* **2006**, *12*, 390–397.
(19) Savini, L.; Gaeta, A.; Fattorusso, C.; Catalanotti, B.; Campiani, G.; Chiasserini, L.; Pellerano, C.; Novellino, E.; McKissic, D.; Saxena, A. Specific targeting of acetylcholinesterase and butyrylcholinesterase recognition sites. Rational design of novel, selective, and highly potent cholinesterase inhibitors. *J. Med. Chem.* **2003**, *46*, 1–4.
(20) Bartolini, M.; Bertucci, C.; Cavrini, V.; Andrisano, V. β-Amyloid aggregation induced by human acetylcholinesterase: inhibition studies. *Biochem. Pharmacol.* **2003**, *65*, 407–416.
(21) Smissman, E. E.; Makriyannis, A. Azodicarboxylic acid esters as dealkylating agents. *J. Org. Chem.* **1973**, *18*, 1652–1657.
(22) Pecherer, B.; Stumpf, J.; Brossi, A. Synthesis and characteristics of various 3-benzazocines, a class of potential analgesics. *Helv. Chim. Acta* **1970**, *53*, 763–770. (German).
(23) Hobson, J. D.; McCluskey, J. G. Cleavage of tertiary bases with phenyl chloroformate: the reconversion of 21-deoxyajmaline into ajmaline. *J. Chem. Soc. C* **1967**, 2015–2017.
(24) Abdel-Monem, M. M.; Porgoghese, P. S. N-Demethylation of morphine and structurally related compounds with chloroformate esters. *J. Med. Chem.* **1972**, *15*, 208–210.
(25) Lu, M. Design and Synthesis of Meptazinol Prodrug and Bivalent Ligands as Analgesics. Ph.D. Dissertation, Fudan University, Shanghai, P. R. China, 2005.
(26) Li, W.; Wang, X.; Lau, C.; Tang, Y.; Xie, Q.; Qiu, Z. Conformational re-analysis of (+)-meptazinol: an opioid with mixed analgesic pharmacophores. *Acta. Pharmacol. Sin.* **2006**, *27*, 1247–1252.
(27) Decker, M.; Krauth, F.; Lehmann, J. Novel tricyclic quinazolinimines and related tetracyclic nitrogen bridgehead compounds as cholinesterase inhibitors with selectivity towards butyrylcholinesterase. *Bioorg. Med. Chem.* **2006**, *14*, 1966–1977.
(28) Nicolet, Y.; Lockridge, O.; Masson, P.; Fontecilla-Camps, J. C.; Nachon, F. Crystal structure of human butyrylcholinesterase and of its complexes with substrate and products. *J. Biol. Chem.* **2003**, *278*, 41141–41147.
(29) Harel, M.; Sussman, J. L.; Krejci, E.; Bon, S.; Chanal, P.; Massoulio, J.; Silman, I. Conversion of acetylcholinesterase to butyrylcholinesterase: modeling and mutagenesis. *Biochem.* **1992**, *89*, 10827–10831.
(30) Greig, N. H.; Lahiri, D. K.; Sambamurti, K. Butyrylcholinesterase: an important new target in Alzheimer's disease therapy. *Int. Psychogeriatr.* **2002**, *14* (Suppl. 1), 77–91.
(31) Birks, J.; Grimley Evans, J.; Iakovidou, V.; Tsolaki, M. Rivastigmine for Alzheimer's disease. *Cochrane Database Syst. Rev.* **2000**, *4*, CD001191.
(32) Bourne, Y.; Radic, Z.; Sulzenbacher, G.; Kim, E.; Taylor, P.; Marchot, P. Substrate and product trafficking through the active center gorge of acetylcholinesterase analyzed by crystallography and equilibrium binding. *J. Biol. Chem.* **2006**, *281*, 29256–29267.
(33) Jones, G.; Willett, P.; Glen, R. C.; Leach, A. R.; Taylor, R. Development and validation of a genetic algorithm for flexible docking. *J. Mol. Biol.* **1997**, *267*, 727–748.
(34) Li, J.; Huang, H.; Miezan Ezoulin, J. M.; Gao, X. L.; Massicot, F.; Dong, C. Z.; Heymans, F.; Chen, H. Z. Pharmacological profile of PMS777, a new AChE inhibitor with PAF antagonistic activity. *Int. J. Neuropsychopharmacol.* **2007**, *10*, 21–29.

(35) Gasteiger, J.; Rudolph, C.; Sadowski, J. Automatic generation of 3D-atomic coordinates for organic molecules. *Tetrahedron Comput. Methodol.* **1990**, *3*, 537–547.
(36) Gasteiger, J.; Marsili, M. Iterative partial equalization of orbital electronegativity—a rapid access to atomic charges. *Tetrahedron* **1980**, *36*, 3219–3228.
(37) Purcell, W. P.; Singer, J. A. Brief review and table of semiempirical parameters used in the Hückel molecular orbital method. *J. Chem. Eng. Data* **1967**, *12*, 235–246.
(38) Clark, R. D.; Strizhev, A.; Leonard, J. M.; Blake, J. F.; Matthew, J. B. Consensus scoring for ligand/protein interactions. *J. Mol. Graphics Modell.* **2002**, *20*, 281–295.
(39) Wang, R.; Lai, L.; Wang, S. Further development and validation of empirical scoring functions for structure-based binding affinity prediction. *J. Comput.-Aided Mol. Des.* **2002**, *16*, 11–26.
(40) Wang, R.; Lu, Y.; Wang, S. Comparative evaluation of 11 scoring functions for molecular docking. *J. Med. Chem.* **2003**, *46*, 2287–2303.
(41) Wallace, A. C.; Laskowski, R. A.; Thornton, J. M. LIGPLOT: a program to generate schematic diagrams of protein—ligand interactions. *Protein Eng.* **1995**, *8*, 127–134.

JM070154Q